MAPPING PROGRESSIVE LAND SUBSIDENCE IN URAYASU CITY, JAPAN, BASED ON MULTI-TEMPORAL DINSAR APPROACH

Yusupujiang Aimaiti, Fumio Yamazaki and Wen Liu

Chiba University, Chiba 263-8522, Japan Email: tuprak100@gmail.com

ABSTRACT: In earthquake-prone areas, identifying ground deformation patterns has great importance before it becomes a latent risk factor. As one of the severely damaged areas due to the 2011 Tohoku, Japan, Earthquake, Urayasu City in Chiba Prefecture has been suffering from land subsidence since a part of its land was built by massive land fill. To investigate long-term land deformation patterns in Urayasu City, three sets of SAR data acquired during the years 1993–2006 from ERS-1/-2 (C-band), 2006–2011 from ALOS PALSAR (L-band) and 2014–2017 from ALOS-2 PALSAR-2 (L-band) were used in conjunction with multi-temporal InSAR techniques. Levelling survey data were also used to verify the accuracy of DInSAR driven results. The results from the ERS-1/-2, ALOS PALSAR and ALOS-2 PALSAR-2 data showed continuing subsidence in several reclaimed areas. The maximum subsidence rate in the period 1993–2006 was up to about 27 mm/year, while in the periods 2006–2011 and 2014–2017 was up to about 30 and 18 mm/year, respectively. The quantitative validation results of the DInSAR driven deformation trend during three observation periods are consistent with the levelling survey data measured from 1993 to 2016.

KEY WORDS: ALOS PALSAR, ENVISAT ASAR, Land Deformation, D-InSAR, PS-InSAR, SBAS-InSAR

1. INTRODUCTION

Land subsidence is one of the most serious environmental problems in many urban areas around the world (Pradhan et al., 2014). Especially the coastal areas which contain young and compressible deposits are often vulnerable to subsidence caused by either anthropogenic or natural factors (Chaussard et al., 2013). Continuous land subsidence causes remarkable economic losses in the damages of buildings and infrastructures with high maintenance costs. Thus, identifying land deformation trends is a crucial task for maintaining the sustainability of urban areas.

Over the past two decades, the land subsidence monitoring has been significantly improved by the utility of Interferometric synthetic aperture radar (InSAR) techniques. Although the traditional methods (i.e., GPS and levelling measurement) can also provide precise measurements, they have certain limitations in achieving large-scale ground displacements, due to required time and cost. Thanks to newly developed advanced time series InSAR techniques, such as persistent scatterer interferometry (PSI) and small baseline subset (SBAS) techniques, they could achieve results in better spatial and temporal resolutions with higher precisions. Furthermore, the increase of available SAR satellites with different temporal and spatial resolutions has provided a great opportunity for researchers to make long-term geohazard monitoring by combining those satellites (Armas et al., 2017).

In this study, we used three sets of SAR data, European Remote Sensing satellites (ERS-1/-2) and Phased Array L-band synthetic aperture radar (PALSAR- & PALSAR-2) onboard the Advanced Land Observation Satellites (ALOS & ALOS-2) to identify the trends of land subsidence dynamics in Uraysu City over a period of 24 years by multi-temporal InSAR techniques. Moreover, the InSAR results were compared with levelling survey data. The observed results may provide useful information in identifying and understanding the behaviour of slow subsidence phenomenon over a long-time period, which plays an important role in the future risk mitigation strategy.

2. THE STUDY AREA AND DATA SETS

Urayasu City locates in the Tokyo Bay area of Chiba Prefecture between E139^{0}56’22’’ to E139^{0}52’20’’ and N35^{0}37’ to N35^{0}40’23’’. The total area is 16.98 km^2 and the total population was 167,950 in 2016. The Urayasu city was divided into three areas, Moto-Machi (old town), Naka-Machi (central town) and Shin-Machi (new town). The Moto-Machi is a naturally formed Holocene lowland, and the other two areas were reclaimed from 1964 to 1980 (Tokimatsu et al., 2013). The elevation in the old coastline area of Moto-Machi is around 0 to 2 m, and it gradually increases toward the coastal levee, especially becomes high in the Sogo Park of Akemi district and Tokyo Disney resort area (Fig. 1). The thickness of alluvial soil layers also varies from 20 m in Moto-Machi area and up to 60-80 m in Naka-Machi and Shin-Machi areas, which indicate the complexity of soft soil distribution in those areas.

In this study, the SAR data collected by the ERS-1/-2 and ALOS-1/-2 satellites were used to monitor the long-term deformation pattern of Urayasu City. The ERS-1/-2

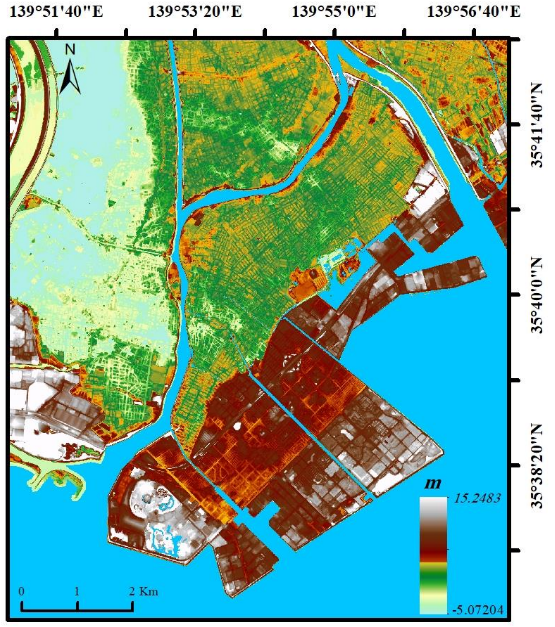

Figure 1. The topography of the study area.

data were provided by the European Space Agency (ESA) and PALSAR & PLASAR-2 data by Japan Aerospace Exploration Agency (JAXA). A total of 52 C-band ERS-1/-2 Single Look Complex (SLC) data were acquired from in the track/frame 489/2889 during the period from November 1992 to March 2006; 24 L-band PALSAR SLC data were acquired from the path/frame 58/2900 during the period from June 2006 to December 2010; 13 L-band PALSAR-2 SLC data were acquired from the path/frame 18/2900 during the period from December 2014 to November 2017.

A 5-m high resolution Digital Elevation Model (DEM) provided by the Geospatial Information Authority of Japan (GSI) was used to remove the topographic phase. The levelling survey measurements have been conducted by the Chiba prefecture every year and the results are publicly available at their official website (Chiba Prefecture, 2018).

3. METHODS

We used two advanced DInSAR time series analysis methods, the persistent scatterer interferometry (PSI) and the small baseline subset (SBAS) to monitor the long-term subsidence in Urayasu City. The PS-InSAR is one of the promising approach that improves the precision of conventional InSAR displacement measurements. The PS-InSAR algorithm utilizes time series of radar images to detect coherent radar signals from PS points in order to derive information of terrain motion (Ferretti et al., 2001). The SBAS algorithm uses conventional interferograms with small baselines to obtain time-series displacements (Berardino et al., 2002). The both algorithms work to minimize the disadvantages of conventional D-InSAR, namely the phase errors due to the geometrical and temporal decorrelations as well as the atmospheric disturbance.

The ERS-1/-2 and PALSAR data were processed using both the PS and SBAS-InSAR methods. Due to the limited number of scenes, the PALSAR-2 data were processed using only the SBAS-InSAR method. For the ERS-1/-2 data, we used the latest precise orbit products provided by the ESA to correct the orbit inaccuracies and generated a total of 424 interferograms including 36 for PS processing and 388 for SBAS processing. The PS-InSAR pairs were generated with respect to the master image of Jan. 24, 2000. The normal baselines range from -22 m to 557 m and the mean coherence threshold of 0.56 was used to identify the PS candidates.

For the PALSAR data, we used both Fine Beam Single (FBS) polarization and Fine Beam Double (FBD) polarization images with HH polarization mode and generated a total of 150 interferograms including 21 for PS processing and 129 for SBAS processing. For the PALSAR-2 data, we generated 78 interferograms for the SBAS-InSAR processing, with respect to the super master image of Dec. 4, 2014. The threshold criteria for the absolute mean of the normal baselines was 182 m and that for the absolute mean of temporal baselines was 386 days. The topographic phases in both the PS and SBAS-InSAR interferograms were removed using the 5-m DEM data.

All the final displacements were measured in the satellite line of sight (LOS) direction, and geocoded in the WGS84 reference ellipsoid with 25 m ground resolution.

4. ANALYSIS RESULTS

4.1 Timeseries Analysis of the ERS-1/-2 Data

The velocity (mm/year) maps of the final geocoded mean displacements generated from the ERS-1/-2 data are shown in Fig. 2 for the PS-InSAR results and Fig. 3 for SBAS-InSAR results. The color cycle from green to purple indicates the positive to negative velocities in the LOS direction. The negative (positive) values indicates the surface is moving away from (close to) the satellite (i.e., subsidence or uplift). As shown in Figs. 2 and 3, the major subsidence areas were highlighted by the purple color from the both InSAR measurements, which were located in the boarders of Naka-Machi and Shin-Machi areas. The results of the SBAS-InSAR measurement show higher density of the obtained points than the ones of the PS-InSAR. In the study area of over 860,256 pixels, 54,458 measurement points were obtained by the PS-InSAR method and 89,251 points by the SBAS-InSAR method, respectively. In general, the ERS-1/-2 measurements show that approximately 85% of the PS points in the study area indicate the displacement rate between -4 mm/year to 2 mm/year.

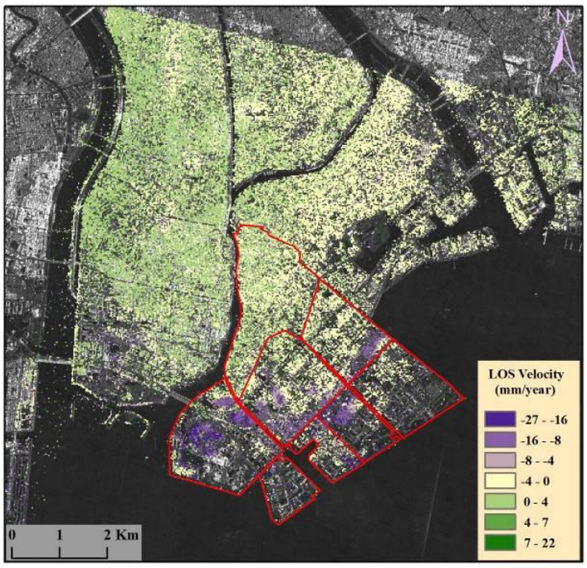

Figure 2. Estimated mean velocity of the LOS displacements from 1993 to 2006 using the PS-InSAR method from the ERS-1/-2 data.

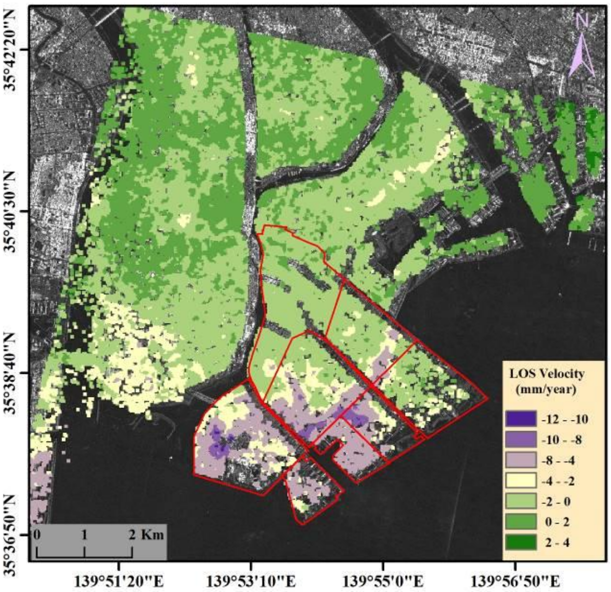

Figure 3. Estimated mean velocity of the LOS displacements from 1993 to 2006 using the SBAS-InSAR method from the ERS-1/-2 data.

4.2 Timeseries Analysis of the PALSAR Data

The mean velocity (mm/year) maps of the displacements for the period from June 2006 to December 2010 is shown in Fig. 4 for the PS-InSAR results and Fig. 5 for SBAS-InSAR results. The same color cycle from green to purple was used for those results. As shown in Figs. 4 and 5, the density of the measured points by the PS-InSAR is coarser than that by the SBAS-InSAR, due to the existence of vegetation in the study area. In the study area of over 695,387 pixels, 50,441 measurement points were obtained by the PS-InSAR method and 78,044 points by the SBAS-InSAR method, respectively. In general, the PALSAR measurements show that approximately 90% of the PS points in the study area indicates a displacement rate between -8 mm/year to 1 mm/year.

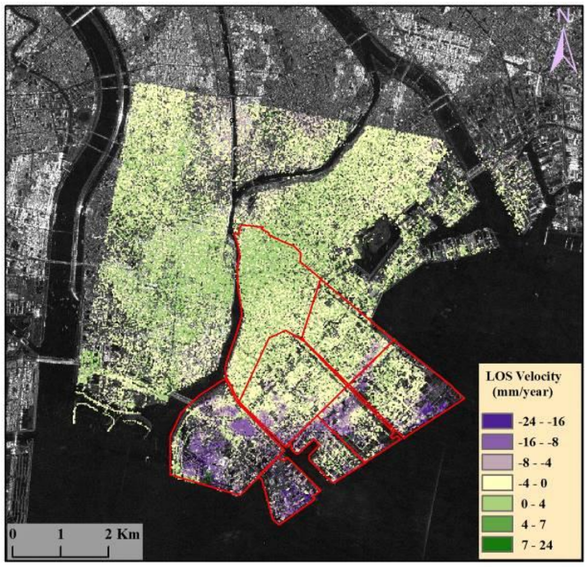

Figure 4. Estimated mean velocity of the LOS displacements from 2006 to 2011 using the PS-InSAR method from the ALOS PALSAR data.

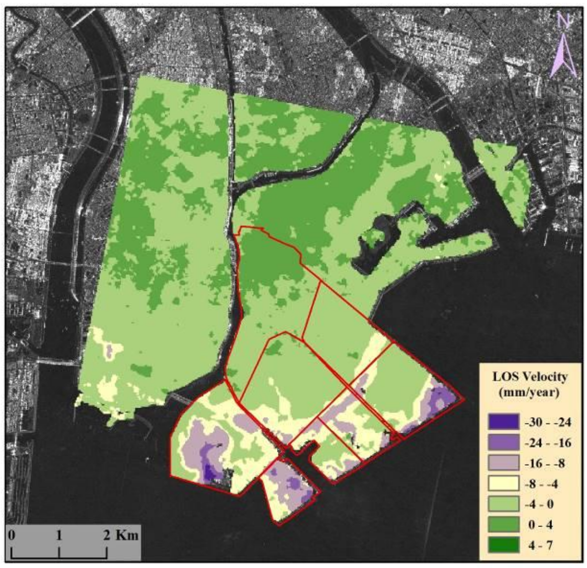

Figure 5. Estimated mean velocity of the LOS displacements from 2006 to 2011 using the SBAS-InSAR method from the ALOS PALSAR data.

4.3 Timeseries Analysis of the PALSAR-2 Data

The mean velocity (mm/year) maps of the displacements for the period from December 2014 to November 2017 is shown in Fig. 6. In the study area of over 690,336 pixels, 76,500 measurement points were obtained by the SBAS-InSAR method. The -0.5 mm/year average displacement rate and the 1.9 mm/year standard deviation were lower than those obtained in the ERS-1/-2 and the PALSAR monitoring period. In general, the PALSAR-2 measurements show that approximately 85% of the PS points in the study area indicate a displacement rate between -3 mm/year to 1.5 mm/year.

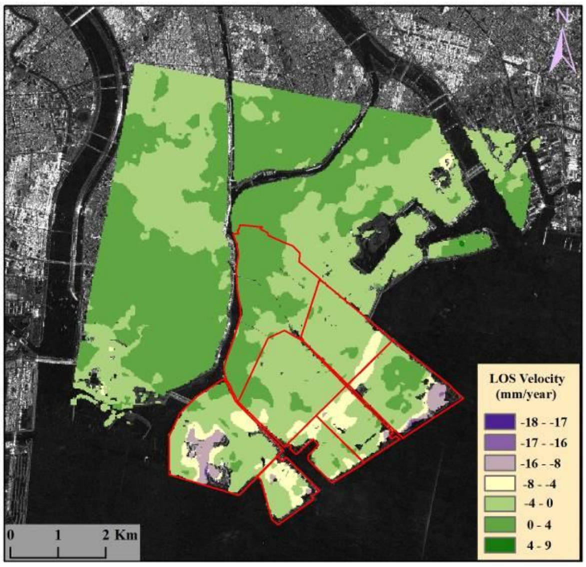

Figure 6. Estimated mean velocity of the LOS displacements from 2014 to 2017 using the SBAS-InSAR method from the ALOS-2 PALSAR-2 data.

4.4 Comparison of InSAR Driven Results and the Levelling Survey Data

In order to assess the accuracy of the InSAR driven results during the three observation periods, a quantitative comparation of the time series displacements with the levelling survey data provided by the Chiba Prefecture at 22 measurement points were performed. We selected the levelling data in the same overlapping periods with the three InSAR measurement periods, respectively. For consistency, the vertical deformations of the levelling data were converted into the LOS directions.

The results show that the root mean square error (RMSE) for the results from the ERS-1/-2 data using the PS and SBAS-InSAR methods were 2.6 mm/year and 4.0 mm/year, respectively. The RMSE for the results from the PALSAR data using the PS- and SBAS-InSAR methods were 2.5 mm/year and 0.9 mm/year. The RMSE for the results from the PALSAR-2 data using the SBAS-InSAR method was 3.3 mm/year. According to these comparisons, the InSAR driven results show a good agreement with the result of the levelling measurements.

5. CONCLUSION

In this study, we used three sets of different SAR data in conjunction with the advanced D-InSAR techniques. The obtained InSAR results during the three observation periods from 1993 to 2014 showed continuing subsidence occurred in several reclaimed areas of Urayasu City. The maximum subsidence rate in the period from 1993 to 2006 was up to about 27 mm/year, in the period from 2006 to 2011 was up to about 30 mm/year, and in the period from 2014 to 2017 was up to about 18 mm/year, respectively. These results were verified by comparing with the levelling survey data. The comparisons showed that the obtained InSAR results have a good agreement to the levelling measurements with a correlation over 0.8. The outcome of this research further implies that the effectiveness of the D-InSAR measurements in the land subsidence monitoring of coastal urban areas.

Acknowledgements

We would like to thank JAXA for providing ALOS-PALSAR and ALOS-2 PALSAR-2 data, and ESA for providing the ER-1/-2 data used in this study.

References

Armaş, I., Mendes, D.A., Popa, R.G., Gheorghe, M. and Popovici, D., 2017. Long-term ground deformation patterns of Bucharest using multi-temporal InSAR and multivariate dynamic analyses: a possible transpressional system?. *Scientific Reports*, 7, p.43762.

Berardino, P., Fornaro, G., Lanari, R., Sansosti, E. 2002. A new algorithm for surface deformation monitoring based on small baseline differential interferograms. *IEEE Transactions on Geoscience and Remote Sensing*, 40(11), 2375–2383.

Chaussard E, Amelung F, Abidin H, Hong S-H. 2013. Sinking cities in Indonesia: ALOS PALSAR detects rapid subsidence due to groundwater and gas extraction. *Remote Sens Environ*, 128:150–161.

Chiba Prefecture. http://www.pref.chiba.lg.jp/suiho/jibanchinka/index.html (Last accessed on 14 March,2018)

Ferretti, A., Prati, C., Rocca, F. 2001. Permanent scatterers in SAR interferometry. *IEEE Transactions on Geoscience and Remote Sensing*, 39, 8–20.

Tokimatsu K, Suzuki H, Katsumata K, Tamura S. 2013. Geotechnical Problems in the 2011 Tohoku Pacific Earthquakes. *International Conference on Case Histories in Geotechnical Engineering*. 2.

Pradhan B, Abokharima MH, Jebur MN, Tehrany MS. 2014. Land subsidence susceptibility mapping at Kinta Valley (Malaysia) using the evidential belief function model in GIS. *Natural Hazards* 73:1019–1042.